

1 ***In silico* Drug Repositioning of bortezomib to reverse metastatic effect of**
2 ***GALNT14* in lung cancer**

3 Running title: **A data-driven route to drug discovery for undruggable targets**

4 Ok-Seon Kwon^{1*}, Haeseung Lee^{2*}, Hyeon-Joon Kong³, Ji Eun Park¹, Woojin Lee¹,
5 Seungmin Kang², Mirang Kim⁴, Wankyu Kim^{2#}, Hyuk-Jin Cha^{1#}

6

7 ¹ College of Pharmacy, Seoul National University, Seoul 08826, Republic of Korea ²
8 Research Center for Systems Biology, Department of Life Sciences, Ewha Womans
9 University, Seoul 03760, Republic of Korea ³ College of Natural Sciences, Department
10 of Life Sciences, Sogang University, Seoul 04107, Republic of Korea SD ⁴Personalized
11 Genomic Medicine Research Center, Korea Research Institute of Bioscience and
12 Biotechnology, Daejeon 34141, Republic of Korea

13 * These authors contributed equally to this work.

14 #Corresponding authors: hjcha93@snu.ac.kr and wkim@ewha.ac.kr

15

16 Hyuk-Jin Cha, PhD

17 College of Pharmacy, Department of Pharmacy, Seoul National University

18 1 Gwanak-ro, Gwanak-gu, Seoul 08826, Republic of Korea

19 Tel.: +82-2-880-7825; Fax: +82-2-880-9122; E-mail: hjcha93@snu.ac.kr

20

21 Wan-Kyu Kim, Ph.D

22 Ewha Research Center for Systems Biology, Department of Life Sciences, Ewha
23 Womans University

24 52, Ewhayeodae-gil, Seodaemun-gu, Seoul 03760 Republic of Korea

1 Tel: +82-2-3277-4132, Fax: +82-2-3277-6809, Email: wkim@ewha.ac.kr

2

3 Conflicts of interest: The author declares that he has no conflict of interest.

1 **Abstract**

2 Although many molecular targets for cancer therapy have been discovered, they
3 often show poor druggability, which is a major obstacle to develop targeted drugs. As
4 an alternative route to drug discovery, we adopted an *in silico* drug repositioning (*in*
5 *silico* DR) approach based on large-scale gene expression signatures, with the goal of
6 identifying inhibitors of lung cancer metastasis. Our analysis of clinoco-genomic data
7 identified GALNT14, an enzyme involved in O-linked N-acetyl galactosamine
8 glycosylation, as a putative driver of lung cancer metastasis leading to poor survival. To
9 overcome the poor druggability of GALNT14, we leveraged Connectivity Map
10 approach, an *in silico* screening for drugs that are likely to revert the metastatic
11 expression patterns. It leads to identification of bortezomib (BTZ) as a potent metastatic
12 inhibitor, bypassing direct inhibition of poorly druggable target, GALNT14. The anti-
13 metastatic effect of BTZ was verified *in vitro* and *in vivo*. Notably, both BTZ treatment
14 and *GALNT14* knockdown attenuated TGF β -mediated gene expression and suppressed
15 TGF β -dependent metastatic genes, suggesting that BTZ acts by modulating TGF β
16 signaling. Taken together, these results demonstrate that our *in silico* DR approach is a
17 viable strategy to identify a candidate drug for undruggable targets, and to uncover its
18 underlying mechanisms.

19

20 **Keywords:** GALNT14, connectivity map, drug repositioning, bortezomib, TGF β ,
21 metastasis, undruggable targets

22

1 **Introduction**

2 In the context of personalized anti-cancer therapy based on targeting specific
3 proteins with the goal of lowering cancer-related mortality (1), a great deal of effort has
4 been devoted to identifying both molecular targets and accompanying drugs (2,3).
5 However, the fraction of patients eligible for personalized anti-cancer therapy is very
6 limited (4) due to the poor druggability of newly identified molecular targets,
7 notwithstanding recent advances in strategies in drugging ‘undruggable’ proteins (5,6).

8 An alternative approach to matching candidate drugs to poorly druggable
9 cancer targets is *in silico* drug repositioning (*in silico* DR) (7,8). Due to the well-
10 characterized pharmacology and safety of approved drug libraries(9), this approach has
11 the potential to reduce cost and attrition during the clinical phases of drug development.
12 Several approaches to DR have been tested in the context of oncology (10) and a few of
13 the resultant drugs, including celecoxib and thalidomide, have been approved by the
14 FDA for repurposing as anti-cancer therapeutics (11). Along with recent advances in
15 sequencing technologies, chemogenomics databases containing drug-induced gene
16 expression profiles provide clues regarding potential treatments for personalized cancer
17 targets, and can also suggest candidate drugs based on tailored gene signatures of
18 cancers upon identification of molecular targets (12). The Connectivity Map (CMap), a
19 collection of genome-wide expression profiles of cell lines treated with >20,000
20 chemicals(13), has been used to identify candidate drugs for certain cancer types
21 (14,15) (16).

22 N-acetyl-galactosaminyltransferases (GalNAc-Ts or GALNTs) are key
23 enzymes that initiate O-linked N-acetyl galactosamine (GalNAc) glycosylation. This
24 process is an important step in the synthesis of Thomsen-nouvelle (Tn) antigens, which

1 are well-characterized tumor-associated molecules (17). In particular, *GALNT14* has
2 been examined in the context of apoptotic signaling (18,19); invasion and migration of
3 breast (20,21), ovary (22), and lung (23) cancers; and multi-drug resistance of breast
4 cancer cells (24). Moreover, *GALNT14* expression is not only a prognostic marker in
5 neuroblastoma (25) and lung cancer (23), but also a predictive marker for
6 Apo2L/TRAIL-based cancer therapy (18), although a randomized phase II study based
7 on the predictive marker of GALNT14 for dulanermin did not improve patient outcome
8 (26).

9 In this study, through transcriptome analysis of the TCGA dataset and *in vitro*
10 and *in vivo* studies, we demonstrated that *GALNT14* is strongly associated with lung
11 cancer recurrence due to the high migration and invasion properties of tumor cells.
12 Rather than attempting direct inhibition of the poorly druggable GALNT14 protein or
13 downstream signaling, we leveraged large-scale drug-induced transcriptome data to
14 identify candidate drug(s) likely to reverse *GALNT14*-dependent gene expression, *i.e.*,
15 drugs that led to transcriptomic changes similar to those induced by *GALNT14* depletion.
16 We successfully identified an anti-metastatic candidate drug that mimicked *GALNT14*
17 depletion. The results demonstrate that this approach represents a viable strategy for
18 discovering candidate drugs for many other undruggable targets.

19

1 **Materials and Methods**

2 **Cell line establishment and Cell culture**

3 H460 cell line which was purchased from Korean cell line bank (KCLB) were
4 maintained in Dulbecco's modified Eagle's medium (DMEM), supplemented with 10%
5 fetal bovine serum (FBS), gentamicin (50 µg/ml) at 37°C in a humidified atmosphere of
6 5% CO₂ in the air. GALNT14 knockdown cell lines with shRNA were established as
7 previously described (23).

8 **Reagents and antibodies**

9 The primary antibodies against cleavage caspase-3 (#9664), cleavage caspase-9 (#9505)
10 and pSmad2 (#310S) were obtained from Cell Signaling Technology. Antibodies
11 against β-Actin (sc-47778), PARP (sc-7150), p53(sc-126), p27 (sc-528), p21 (sc-397),
12 CyclinD1(sc-718) and CyclinB1 (sc-245) were obtained from Santa Cruz
13 Biotechnology Inc. and β-catenin (BD 610153) was purchased from BD Biosciences
14 pharmigen. Bortezomib (S1013) and Carfilzomib (S2853) were purchased from
15 selleckchem.

16 **RNA-sequencing and analysis**

17 Total RNA was isolated using the Trizol according to the manufacture instruction. For
18 library construction, we used the TruSeq Stranded mRNA Library Prep Kit (Illumina,
19 San Diego, CA). Briefly, the steps of strand-specific protocol are: first strand cDNA
20 synthesis; second strand synthesized using dUTPs instead of dTTPs; end repair, A-
21 tailing, and adaptor ligation; PCR amplification. Then, each library was diluted to 8
22 pM for 76 cycles of paired-read sequencing (2 X 75bp) on the Illumina NextSeq 500 per
23 the manufacturer's recommended protocol.

24 **TCGA data processing and analysis**

1 TCGA lung adenocarcinoma (LUAD) cohort (n=576), containing mRNA gene
2 expression and clinical data on 388 primary lung cancers, 128 lung cancers with
3 recurrence, and 59 benign lung tissues were collected from the Broad GDAC Firehose
4 (<https://gdac.broadinstitute.org/>). Total 494 patients with clinical information tracked
5 for at least one month were used for survival analysis. For 20,531 genes, all patients
6 were divided into high and low groups by the median expression of each gene and
7 relapse-free survival analysis was performed according to the group difference. Hazard
8 ratio and *P* value were calculated by Cox proportional hazards regression model and
9 log-rank test respectively. With 58 patients who have gene expression profiles of
10 normal benign tissues, differential expression in LUAD compared to matched normal
11 samples were measured from the likelihood ratio test. RNA-seq profiles were
12 normalized and processed using R package ‘limma’ and ‘DESeq2’ and survival analysis
13 was conducted by R package ‘survival’.

14 **Metastasis and Tumorigenesis signatures**

15 From MSigDB manually curated gene sets (C2), we collected the 35 metastasis- and
16 44 tumor-related gene sets that are annotated by ‘metastasis’ / ‘epithelial-mesenchymal
17 transition’ and ‘cancer’/ ‘tumorigenesis’, respectively. We took only Up-regulated
18 genes when both UP- or DOWN-regulated sets were available. Then, we selected 32
19 and 23 genes as the metastatic and the tumorigenesis signature, respectively, by taking
20 the consensus genes common to at least three or more gene sets.

21 **Anti-metastatic drug prediction using CMap dataset**

22 The updated CMap, or LINCS L1000(13), provides an extensive catalog of >1.2 million
23 transcriptome signatures from 71 human cell lines in response to each of 20,413 small
24 molecule treatments and are different from the original CMap based on the

1 microarray(27). This dataset contains multiple expression signatures even for the same
2 drug and cell line depending on dose, sample time, and batch. Therefore, we developed
3 our own DR method to handle such redundancy, which is distinct from the original
4 CMap method based on rank-based Kolmogorov-Smirnov (KS) test. Differential gene
5 expression matrix (level 5, replicate-collapsed z-score) and metadata were obtained
6 from the Gene Expression Omnibus (accession id: GSE92742). Each column in the
7 matrix represents an experiment consisting of chemical perturbation in a cell line, and
8 each row represents a gene whose degree of differential expression was quantified in
9 that experiment, respectively. After filtering out the experiments which consist of less
10 than three replicates and low-quality ($\text{distil_cc_q75} < 0.2$, and $\text{pct_self_rank_q25} > 5$),
11 the 100 most up- and down-regulated genes were selected as the expression signature of
12 an experiment. Given a set of genes representing a specific phenotype, a series of gene
13 set analysis toward gene signatures of all experiments was performed using *Jaccard*
14 *index*. After calculating the similarities, multiple similarity scores of a compound are
15 combined into a single score, drug-repositioning (DR) score. DR score is defined as the
16 negative logarithm of the *P*-value of hypergeometric test that quantifies the degree of
17 over-representation of experiments of a compound within the top 10% of similarity
18 scores.

19 **GALNT14-TGF β signature**

20 TGF β downstream target genes (39 SMAD4 dependent genes and 65 SMAD4
21 independent genes) were collected from the literature (28). Among the SMAD4
22 dependent targets, a set of genes commonly down-regulated by both BTZ and sh*GAL*
23 (*ATF3*, *ARNTL*, *COPA*, *NEDD9*, *LAMC2*, *RAB27B*, and *PCDH7*) was defined as
24 ‘*GALNT14*–TGF β signature’. To measure the average activity of the signature, KS

1 statistic was used to estimate the degree of up- or down-regulation of the seven genes in
2 a sample's gene expression profile. In TCGA LUAD cohort, the patients with activity in
3 the top 10% (n=50) or lower 10% (n=50) were classified as 'high' or 'low' respectively.

4

5 **Statistical analysis**

6 The graphical data were presented as mean \pm S.E.M. Statistical significance among the
7 three groups and between groups was determined using one-way or two-way analysis of
8 variance (ANOVA) following Turkey post-test and Student's t-test respectively.

9 Significance was assumed for $p < 0.05$ (*), $p < 0.01$ (**), $p < 0.001$ (***)).

10

1 Results

2 *GALNT14* as a putative molecular target for lung cancer metastasis

3 Identification of molecular targets in recurrent cancers is essential not only for
4 predicting prognosis, but also for matching specific drug–target pairs if they are
5 available. To identify potential molecular targets related to cancer recurrence, we
6 assembled transcriptome data and clinical information from 516 lung cancer patients
7 from the TCGA LUAD cohort (Fig. 1A). Concentrating on molecular targets relevant to
8 recurrent lung cancer, we performed a series of relapse-free survival (RFS) analyses and
9 differential expression analyses. Expression of seven genes (*GALNT14*, *COL7A1*,
10 *GPR115*, *CIQTNF6*, *KRT16*, *INHA*, and *TNFSF11*) was significantly associated with
11 cancer progression, recurrence (Fig. 1B), and overall survival (Fig. S1A), indicating that
12 these genes are potentially valuable as predictors of poor prognosis. Notably,
13 metastasis-related genes were significantly overrepresented in gene lists selected by
14 both RFS ($P = 2.3 \times 10^{-6}$) and differential expression ($P = 5.2 \times 10^{-19}$) analysis,
15 including two genes (*e.g.*, *TNFSF11* and *INHA*) among the seven aforementioned
16 candidates. To further confirm the relevance of each gene to metastasis or tumorigenesis,
17 we divided lung cancer patients into two groups (low or high) using the median
18 expression of each gene as the cutoff. Both metastasis and tumor signatures were
19 positively enriched in the high-expression groups of all seven genes (Fig. 1C), and the
20 significant enrichment was observed for *GALNT14* (Fig. 1D).

21 *GALNT14*, which encodes a glycosyltransferase involved in O-glycosylation,
22 has been implicated in both tumor malignancy (25) and metastasis (20,21,23). As
23 expected, metastatic (Fig. 1E) and tumorigenic potentials (Fig. 1F) were markedly
24 attenuated by loss of *GALNT14*, indicating that the gene is important for metastasis as

1 well as tumorigenesis. Further, metastatic lung cancer cells were more vulnerable to
2 *GALNT14* depletion than non-metastatic or other types of cancers in the *Project*
3 *Achilles* dataset(29), a genome-scale RNAi screening data from for 501 cancer cell lines,
4 including 126 cell lines originating from metastatic patients (Fig. 1G). Other candidate
5 genes were less vulnerable in metastatic lung cancer (Fig. S1B). Consistent with this,
6 *GALNT14* expression shows a clearly negative correlation with both locoregional
7 recurrence-free survival (LRFS) and distant metastasis-free survival (DMFS) (Fig. 1H)
8 as well as overall survival (Fig. S1A) in the TCGA LUAD cohorts. In addition, normal
9 lung expresses only a low level of *GALNT14*, and there is a large gap between normal
10 and lung cancer tissue (Fig. S1C)(30). All these results suggested *GALNT14* as a
11 promising molecular target for lung cancer metastasis to improve patient survival.

12

13 **Computational repositioning of BTZ to reverse the *GALNT14* expression signature**

14 Although *GALNT14* may be a potential therapeutic target for metastatic lung cancer,
15 GALNTs remain poorly druggable despite several attempts to find specific inhibitors
16 (31,32). Notably in this regard, GALNT14-dependent metastatic potential is governed
17 by induction of transcription factors (e.g. *HOXB9* or *SOX4*) rather than by altered
18 glycosylation (20,23). Therefore, rather than inhibiting *GALNT14* directly, we leveraged
19 the CMap dataset to virtually screen for drugs that mimic the effect of *GALNT14*
20 depletion at the transcriptome level. To this end, we generated two gene signatures: (i)
21 73 genes down-regulated in the *GALNT14*-low vs *GALNT14*-high group in the TCGA
22 LUAD cohort, and (ii) 129 genes down-regulated by *GALNT14* knockdown in the H460
23 cell line. Next, we collected a comprehensive list of (iii) 3711 metastasis-related genes.
24 Finally, we refined the gene signatures (i, ii) to 20, and 49 genes as *GALNT14*

1 signatures by taking common genes with the genes of (iii). Accordingly, our subsequent
2 predictions would prioritize drugs that may be relevant to both *GALNT14*-dependence
3 and metastasis, but irrelevant genes tend to be filtered out.

4 Using the two *GALNT14* signatures, we performed two independent predictions by
5 CMap analyses (Fig. 2A). Candidate drugs were prioritized according to their DR
6 scores (See Materials and Methods in detail). Two drugs, dexamethasone (DEX, an
7 anti-inflammatory corticosteroid) and bortezomib (BTZ, a first-in-class proteasome
8 inhibitor used to treat multiple myeloma), were among the top ten candidates in both
9 predictions. We then validated expression levels of *SOX4*, *AREG*, and *VCAN*, which are
10 strongly associated with metastasis and regulated by *GALNT14* (20,23) (Figs. S2B and
11 S2C). Among genes differentially expressed in response to either DEX or BTZ in the
12 CMap dataset, *SOX4* (but not *AREG* or *VCAN*) was commonly altered, indicating that
13 *SOX4* could serve as a validation marker (Fig. S2C). As predicted, we observed dose-
14 dependent suppression of *SOX4* (but not *VCAN*) in H460 cells treated with either DEX
15 or BTZ. Although BTZ suppressed *SOX4* less effectively than DEX (EC₅₀: 15 nM vs. 5
16 nM, respectively) (Fig. S2D), BTZ treatment led to a significant reduction in the
17 migration capacity of H460 cells, whereas DEX did not (Fig. 2C). The EC₅₀ for
18 proteasome inhibition was around 20 nM (Fig. 2D and S2E), a concentration at which
19 BTZ clearly inhibited migration (Figs. 2E and S2F) and invasion (Fig. 2F) by lung
20 cancer cells, while it did not affect *GALNT14* expression (Fig. S2G), cell viability (Figs.
21 2G and S2H) nor the cell proliferation (Figs. 2H and S2I). Of note, H358 with relatively
22 lower *GALNT14* expression than H1299 and H460 did not respond to BTZ treatment in
23 migration (Fig. S2K) and invasion (Fig. S2L) unlike H1299, while proteasome
24 inhibition by BTZ occurred (Fig. S2M), suggesting that anti-invasion/migration effect

1 of BTZ would be associated with GALNT14 expression.

2

3 **The effect of BTZ is independent of proteasome inhibition**

4 Given that the anti-migration/invasion effect of BTZ occurred at a
5 concentration that also inhibited proteasome activity (Figs. 2D and E), we sought to
6 determine whether this effect was a result of proteasome inhibition *per se*. To
7 investigate this issue, we first compared the chemical structure of three FDA-approved
8 proteasome inhibitors, BTZ, carfilzomib (CFZ), and ixazomib (IXZ), all of which are
9 approved for treatment of multiple myeloma (33). CFZ (but not IXZ) was structurally
10 similar to BTZ as calculated by Tanimoto coefficient or Jaccard index of molecular
11 fingerprints(34) (Fig. 3A). In contrast to BTZ, the concentration of CFZ that inhibited
12 proteasome activity (Fig. S3A) and stabilized well-characterized proteasome targets β -
13 catenin, Cyclin D1, and p27 (Fig. 3B) failed to suppress migration (Fig. 3C) and
14 invasion (Fig. 3D). Moreover, the boronic acid moiety responsible for the proteasome
15 inhibition (35) was present in both BTZ and IXZ. However, like CFZ, treatment with
16 IXZ could not inhibit migration (Fig. S3B). These data suggest that BTZ has an off-
17 target effect that is independent of proteasome inhibition.

18 To confirm that the anti-migration/invasion effect of BTZ is not dependent on
19 proteasome inhibition, we compared transcriptome profiles of H460 cells treated with
20 BTZ, CFZ and depleted of *GALNT14* (sh*GAL*). Perturbation by BTZ and sh*GAL* (but
21 not CFZ) induced similar transcriptomic changes relative to the control (Fig. 3E).
22 Moreover, the expression patterns of metastatic signature genes were even more similar
23 between BTZ and sh*GAL*, whereas CFZ had a minimal effect on only a few genes (Fig.
24 3E, middle panel). By contrast, expression of proteasome-related genes was altered

1 significantly by both drugs, but only marginally by *shGAL* (Fig. 3E, right panel). Genes
2 down-regulated by BTZ and *shGAL* overlapped significantly (101 common genes; $P =$
3 5.3×10^{-54}), suggesting that BTZ treatment partially mimics depletion of *GALNT14* (Fig.
4 3F). These results are consistent with the phenotypic outcomes, i.e., BTZ, but not CFZ,
5 suppressed cell migration and invasion similarly to *GALNT14* depletion.

6

7 **Attenuation of the TGF β gene response by BTZ treatment or GALNT14** 8 **knockdown**

9 We hypothesized that a subset of the 101 genes down-regulated by both BTZ
10 treatment and *GALNT14* depletion could account for anti-migration/invasion effects of
11 BTZ. To investigate the drug's mode of action, we conducted pathway enrichment
12 analysis of the 101 genes and investigated the clinical significance of each pathway (Fig.
13 4A). Among the most enriched pathways was TGF β signaling (hazard ratio [HR] = 1.2).
14 BTZ treatment induced changes in expression of individual TGF β signaling genes that
15 were very similar to those induced by *shGAL* (Fig. S4A for BTZ and Fig. S4B for
16 *shGAL*). Moreover, genes commonly down-regulated (e.g., *INHBA*, *FST*, and *BMPR*)
17 among targets of TGF β signaling were indeed suppressed (Fig. 4B). Suppression of the
18 TGF β -dependent gene signature, a common effect of BTZ treatment and *GALNT14*
19 depletion, was validated by reporter assays using the Smad-binding element (SBE),
20 activin-response element (ARE), and BMP-response element (BRE) (Fig. 4C).
21 Similarly, TGF β reporter activity decreased after treatment with BTZ, but not CFZ (Fig.
22 4D), while β -catenin and Cyclin D1 were stabilized by proteasome inhibition following
23 treatment with either BTZ or CFZ (Fig. 4E). Concomitant with the reduction in Smad2

1 phosphorylation with (Fig. 4E) or without TGF β stimulation (Fig. S4C), SMAD4
2 nuclear translocation was inhibited significantly by BTZ treatment (Fig. 4F).
3 Consistently, TGF β dependent gene responses (determined by SBE or BRE) upon
4 TGF β stimulation, were significantly attenuated by BTZ treatment (Fig. S4D). As
5 depletion of SMAD4 was sufficient to inhibit both migration and invasion (Figs. 4G and
6 H), inhibition of SMAD2 phosphorylation (Figs. 4E and S4C) and subsequent delay of
7 SMAD4 nuclear translocation (Fig. 4F) by BTZ would be a possible mode of action of
8 BTZ. It is important to note that the TGF β signaling pathway has been studied
9 extensively as a tumor suppressor, a tumor promoter (36), and a promoter of metastasis
10 (37). To determine whether the TGF β signaling response is associated with *GALNT14*,
11 we selected a set of TGF β downstream targets (28) and examined their correlations with
12 *GALNT14* expression and patient prognosis (Fig. 4I). Notably, SMAD4-dependent
13 targets *PCDH7* and *LAMC2*, previously shown to induce metastasis (38,39) or
14 tumorigenicity (40,41), were highly correlated with *GALNT14* (Fig. 4I). Moreover, the
15 SMAD4-dependent TGF β targets was associated to RFS in the *GALNT14*-high group (P
16 = 0.045, Fig. 4J), suggesting that some SMAD4-dependent targets responsible for
17 cancer recurrence are strongly associated with *GALNT14* expression. These results
18 imply that BTZ treatment, like *GALNT14* depletion, exerts its anti-metastatic effect by
19 interfering with nuclear translocation of SMAD4 (Fig. 4F) and with the SMAD4-
20 dependent gene expression response (Fig. 4D). Finally, we defined a set of genes
21 commonly down-regulated by both BTZ and sh*GAL* among the SMAD4 dependent
22 targets as ‘*GALNT14*-TGF β signature’ (See Materials and Methods). The average
23 activity of the *GALNT14*-TGF β signature strongly discriminated patient RFS ($P = 4.0 \times$

1 10^{-4} , Fig. 4K), and *GALNT14* expression was significantly higher in lung cancer
2 patients with higher levels of the signature ($P = 0.025$, Fig. 4L). Overall, these results
3 suggest that suppressing TGF β signaling and gene expression responses relevant to
4 BTZ (similar to the response observed after *GALNT14* depletion) makes a major
5 contribution to reducing migration and invasion.

6

7 ***In vivo* validation of ant-metastatic effect of BTZ**

8 Given the anti-migration/invasion effect of BTZ in a lung cancer cell model (Fig. 2), we
9 next tested the *in vivo* efficacy of BTZ against cancer metastasis *in vivo*. For this
10 purpose, local metastasis was induced in mice by tail vein injection of H460 lung cancer
11 cells, followed by treatment with or without BTZ or CFZ twice weekly for three weeks
12 (Fig. 5A). The proteasome-inhibitory effect of BTZ (0.1mg/kg) with CFZ (0.5 mg/kg)
13 was examined by measuring proteasome activity in blood (Fig. 5B). Under this
14 concentration, the mice tolerated both BTZ and CFZ, exhibiting neither significant loss
15 of body weight nor any other abnormalities (Fig. 5C). Consistent with the *in vitro* assay,
16 the number of metastatic nodules in the lungs of BTZ-treated mice was significantly
17 lower than that in CFZ- or vehicle-treated animals (Fig. 5D and S5A). Close
18 examination of cancer tissue also revealed that inflammatory lesions, which provide
19 favorable microenvironments for tumor formation (42), were present in both CFZ- and
20 vehicle-treated mice (Fig. S5B). Taken together, the *in vivo* and *in vitro* data reveal that
21 BTZ has a significant therapeutic advantage over CFZ in that it inhibits cancer
22 metastasis without significant undesirable side effects.

23

1 Discussion

2 Although many molecular targets for tumorigenesis and metastasis have been
3 identified, most remain undruggable. For example, the GALNTs, expression of which is
4 strongly associated with various properties of cancer (20,21) (22-25), have yet to be
5 drugged, although a few attempts have been made to develop inhibitors of GALNT-
6 dependent O-linked glycosylation (31,32). Thereby, instead of searching direct
7 inhibitors of GALNT14, we adopted an *in silico* DR approach to reverse the *GALNT14*-
8 dependent metastatic expression signature with the goal of finding a candidate drug that
9 could interfere with the *GALNT14*-dependent cancer phenotype. Notably, *HOXB9* and
10 *SOX4*, transcription factor genes regulated by *GALNT14*, are responsible for metastasis
11 (23) and self-renewal (20), respectively, suggesting that downstream transcriptional
12 modulation would be a promising strategy.

13 Unlike similar studies in the past that used the CMap method to analyze differences
14 in gene expression signatures between normal and cancerous tissue (14,43), we focused
15 exclusively on genes (e.g., *GALNT14*) related to the pertinent phenotype (*i.e.*, the
16 metastatic gene signature) (Fig. 1) and identified BTZ as a drug candidate with novel
17 anti-metastatic effects both *in vitro* (Fig. 2C–2H) and *in vivo* (Fig. 5). Importantly, we
18 also demonstrated that the anti-metastatic effect of BTZ, in contrast to that of CFZ, was
19 independent of proteasome inhibition (Fig. 3). Moreover, the metastatic gene signature
20 of CFZ was also distinct from that of BTZ, whereas the proteasome gene signatures of
21 the two drugs were relatively similar (Fig. 3). Recent studies examined the inhibitory
22 effect of BTZ on TGF β -dependent responses such as fibrosis (44) and survival of
23 lymphoma (45), and the results support our conclusions. We also identified the
24 *GALNT14*-TGF β signature that serves as clear indicators of poor prognosis (Fig. 4).

1 Thus, attenuation of TGF β signaling by BTZ, depletion of *GALNT14*, or inhibition of
2 TGF β signaling all decrease invasive properties *in vitro* (Fig. 4) and lung metastasis *in*
3 *vivo* (Fig. 5), suggesting the drug's mode of action. Accordingly, the *GALNT14*-TGF β
4 signature represents potentially useful prognostic marker for lung cancer patients, and
5 could be used alongside previously reported marker [*e.g.*, the TGF β -response signature
6 (TBRS) (46) and the MAPK pathway activity score (MPAS) (47)]. Of note, although
7 BTZ had no undesirable side effects in our *in vivo* experiments, the risk of peripheral
8 neuropathy in patients treated with BTZ (48) merits a further search for other candidate
9 drugs with safer profiles that could also reverse the gene signature associated with
10 *GALNT14* or *GALNT14*-TGF β activity. The continued search for improved candidates
11 could be performed using recently reported *in silico* (or computational) DR tools
12 (8,49,50). Notably in this regard, a recent *in silico* approach can predict candidate drugs
13 capable of modulating the activities of oncogenic transcription factors, a class of
14 proteins that has yet to be drugged (7). In the future, it would be interesting to apply this
15 type of approach to modulate *GALNT14*-regulated transcription factor genes such as
16 *HOXB9* and *SOX4*, which mediate metastasis (23) and self-renewal (20), respectively.

17 Besides predicting potential candidate drugs, our *in silico* DR approach enabled
18 identification of several marker genes that turned out to be strongly associated with
19 clinical outcomes such as RFS. This strategy, which integrated multiple independent
20 expression signatures from cancer patients, genetic perturbation (*e.g.*, knockdown or
21 overexpression), and drug treatment (CMap), would be applicable generally to any other
22 types of target. Thus, our results provide a strong “proof-of-concept” that our DR
23 method is a viable strategy for accessing undruggable molecular targets, leading to
24 identification of candidate drugs that target specific cellular processes such as cancer

1 metastasis.

2

3 **SUPPLEMENTARY DATA**

4 Supplementary Data are available at NAR online.

5

6 **ACKNOWLEDGEMENT**

7 We appreciate Jeong-Hwan Kim, Seon-Young Kim and Dong-Uk Kim at Korea
8 Research Institute of Bioscience and Biotechnology (KRIBB) for helpful discussions.

9

10 **FUNDING**

11 This work was supported by a grant from the National Research Foundation of Korea (
12 NRF-2017M3C9A5028691 and NRF-2017M3A9B306184 from HJ.C and NRF-2017
13 M3A9B3061843 from W.K).

14

15 **DISCLOSURE DECLARATION**

16 The authors declare that they have no conflict of interest.

17

18 **Authors' contributions**

19 HJ.C and W.K conceived the overall study design and led the experiments. OS.K and
20 H.L mainly conducted the experiments, data analysis, and critical discussion of the
21 results. HJ.K, JE.P, and W.L conducted the mouse xenograft experiments. S.K, JH.K
22 and M.K generated RNAseq data performed analysis. All authors contributed to
23 manuscript writing and revising, and endorsed the final manuscript.

24

25

1 **Figure Legends**

2 **Figure 1 *GALNT14* as a putative molecular target for lung cancer metastasis**

3 **A.** Identification of therapeutic targets for both cancer progression and recurrence based
4 on transcriptomic analysis of lung cancer patients. **B.** Selection of therapeutic target
5 candidates that are differential expressed between tumor and normal tissue as well as
6 significantly associated to RFS in the 516 patient dataset from TCGA LUAD. Red
7 circles indicate metastasis-related genes annotated by MSigDB. **C.** Enrichment analysis
8 of metastatic and tumor signatures between high- and low-expressed patient groups for
9 each of the seven candidate genes. **D.** The normalized enrichment score (NES) was
10 calculated by Gene Set Enrichment Analysis (GSEA) for the metastasis (left) and
11 tumorigenesis signature (right) after all the genes were ranked by their expression fold
12 change. **E-F.** 1×10^6 control H460 (shCont) and *GALNT14* knockdown (shGal) cells
13 were injected into lateral tail vein (E) or flanks (F) of nude mice. The representative
14 H&E staining images of tumor-bearing lung (E) and tumors (F) were presented. **G.**
15 Comparison of *GALNT14* dependencies among metastatic and primary cell lines from
16 lung and other types of cancer from the *Project Achilles* dataset. Only metastatic lung
17 cells show a significant dependency on *GALNT14*. **H.** Comparison between the high-
18 and low- expression group for *GALNT14* in terms of locoregional recurrence-free
19 survival (LRFS), and distant metastasis-free survival (DMFS) in LUAD patients.

20 **Figure 2 Computational repositioning of BTZ to reverse the *GALNT14* expression**
21 **signature**

22 **A.** CMAP analyses to prioritize anti-metastatic candidate drugs using the two
23 independent *GALNT14* signatures. Candidate drugs were prioritized according to the
24 similarities between drug-induced down-DEGs and the two *GALNT14* signatures. **B.**

1 DR score of top candidate drugs selected by the *GALNT14* signatures from TCGA (x-
2 axis) and H460 (y-axis). The two drugs marked in red (dexamethasone and bortezomib)
3 got high scores in both predictions. **C.** Cell migration rate after treatment of BTZ and
4 DEX respectively was measured. Representative images (left) and quantification graph
5 (right) were exhibited **D.** Proteasome activity with IC50 concentration in H460 cell line
6 was measured after indicated dose of BTZ treatment **E.** IC50 value of BTZ on cell
7 migration capacity was measured in H460 cell line (right). Recovery ratio was measured
8 43 hours after BTZ treatment and representative image was shown (left). **F.**
9 Representative image of cell, which is invaded through trans-well membrane was
10 shown (left) and quantification of invaded area was presented (right). **G.** Flow
11 cytometry plot (upper) of Annexin V and 7-AAD staining 24 hours after BTZ treatment
12 (indicated concentration) and the quantification graph (lower) of cell death population
13 were presented. **H.** Propidium iodide (PI) was stained to analyze the cell cycle profiles
14 after BTZ treatment. Flow cytometry plot (left) and quantification graph of population
15 in each cell cycle phase (right) were presented.

16 **Figure 3 The effect of BTZ is independent of proteasome inhibition**

17 **A.** Chemical structure of proteasome inhibitors (bortezomib, carfilzomib, and ixazomib)
18 and their Tanimoto similarity heatmap. Red circle indicates the boronic acid structure. **B.**
19 Immunoblotting for β -catenin, Cyclin D1 and p27 after treatment of BTZ (20 nM) and
20 CFZ (20 nM) and α -tubulin for equal protein loading control **C.** Cell migration ratio
21 were measured after 48 hours with 20nM of BTZ and CFZ treatment **D.** Area of cells,
22 invaded through trans-well membrane was measured at 24 hour after treatment of BTZ
23 and CFZ (20 nM) **E.** Sample clustering using t-SNE based on the expression of whole
24 genes, metastasis-related genes and proteasome-related genes. Each sample was colored

1 according to its perturbation type. **F.** Venn diagram of differentially down-regulated
2 genes by BTZ, CFZ and sh*GAL* perturbation in the gene space of whole genes.

3 **Figure 4 Attenuation of the TGF β gene response by BTZ treatment or GALNT14**
4 **knockdown**

5 **A.** Significantly enriched pathways using the 101 genes (hypergeometric test, *P* value <
6 0.01 and FDR < 0.1) and the distribution of each of their RFS HR in TCGA LUAD
7 cohort. The red circle represents the median of HR, and the bar across the circle
8 represents the range of HR. **B.** mRNA expression of 10 common differentially
9 expressed genes with loss of GALNT14 and BTZ treatment. **C.** The activity of
10 TGF β /Smad signaling in H460 shCont and H460 shGal was determined with SBE, ARE
11 and BRE luciferase reporter systems. Luciferase activity was measured and its fold
12 induction is shown as a graph. **D.** BRE luciferase activity was measured at 24 hours
13 after BTZ and CFZ treatment. **E.** Protein level of Smad2 (pSmad2) and ERK2 (pERK2)
14 phosphorylation were measured by immunoblotting 24 hours after BTZ and CFZ
15 treatment. β -actin used as an equal protein loading control. **G-H** Wound healing assay
16 (G) and Two-chamber invasion assay (H) were performed after TGF β signaling
17 suppression with siRNA targeting SMAD4 (siSMAD4). **I-L.** Analysis of TCGA LUAD
18 cohort, **I.** The relationships between correlation score with *GALNT14* expression (z-
19 transform of Spearman correlation, x-axis) and RFS HR (y-axis) of each gene in TGF β
20 target genes. The dependency of TGF β target genes on Smad4 was labeled with two
21 different colors (yellow: Smad4-dependent, blue: Smad4-independent). **J.** KM plot of
22 RFS stratified by the combination of *GALNT14* expression (low and high) and TGF β
23 target activity (low and high). TGF β target activity was measured using SMAD4
24 dependent genes (left) and independent genes (right) individually. Significant

1 differences between the patient groups were marked with the asterisk (*). **K.** KM plot of
2 RFS stratified by the *GALNT14*-TGF β signature. *P* values and HR were calculated with
3 the log-rank test and Cox regression, respectively. **L.** Differences in *GALNT14*
4 expression by *GALNT14*-TGF β signature in TCGA LUAD cohort. *P* values were
5 calculated with Student's t-test.

6 **Figure 5 *In vivo* validation of anti-metastatic effect of BTZ**

7 **A.** Schematic overview of *in vivo* experimental procedure **B.** Proteasome activity with
8 whole blood collected 1 hour after BTZ (0.1 mg/kg) or CFZ (0.5 mg/kg) was shown in a
9 bar graph. **C.** Body weight of each mouse, measured twice in a week was shown at
10 indicative days. **D.** Representative lung image of each group was shown. White
11 arrowheads indicate tumor nodule (top panels). Number of tumor nodules in the lung at
12 each condition was shown in the table (bottom panel) **E.** H&E staining of lung from
13 tumor-bearing mice after treatment of BTZ and CFZ

14

1 References

- 2 1. Spear, B.B., Heath-Chiozzi, M. and Huff, J. (2001) Clinical application of
3 pharmacogenetics. *Trends Mol Med*, **7**, 201-204.
- 4 2. Olsen, D. and Jorgensen, J.T. (2014) Companion diagnostics for targeted cancer
5 drugs - clinical and regulatory aspects. *Front Oncol*, **4**, 105.
- 6 3. Kim, E.S., Herbst, R.S., Wistuba, II, Lee, J.J., Blumenschein, G.R., Jr., Tsao, A.,
7 Stewart, D.J., Hicks, M.E., Erasmus, J., Jr., Gupta, S. *et al.* (2011) The BATTLE
8 trial: personalizing therapy for lung cancer. *Cancer Discov*, **1**, 44-53.
- 9 4. Marquart, J., Chen, E.Y. and Prasad, V. (2018) Estimation of The Percentage of
10 US Patients With Cancer Who Benefit From Genome-Driven Oncology. *JAMA*
11 *Oncol*.
- 12 5. Lazo, J.S. and Sharlow, E.R. (2016) Drugging Undruggable Molecular Cancer
13 Targets. *Annu Rev Pharmacol Toxicol*, **56**, 23-40.
- 14 6. Dang, C.V., Reddy, E.P., Shokat, K.M. and Soucek, L. (2017) Drugging the
15 'undruggable' cancer targets. *Nat Rev Cancer*, **17**, 502-508.
- 16 7. Gayvert, K.M., Dardenne, E., Cheung, C., Boland, M.R., Lorberbaum, T.,
17 Wanjala, J., Chen, Y., Rubin, M.A., Tatonetti, N.P., Rickman, D.S. *et al.* (2016)
18 A Computational Drug Repositioning Approach for Targeting Oncogenic
19 Transcription Factors. *Cell Rep*, **15**, 2348-2356.
- 20 8. Nagaraj, A.B., Wang, Q.Q., Joseph, P., Zheng, C., Chen, Y., Kovalenko, O.,
21 Singh, S., Armstrong, A., Resnick, K., Zanotti, K. *et al.* (2018) Using a novel
22 computational drug-repositioning approach (DrugPredict) to rapidly identify
23 potent drug candidates for cancer treatment. *Oncogene*, **37**, 403-414.
- 24 9. Ashburn, T.T. and Thor, K.B. (2004) Drug repositioning: identifying and
25 developing new uses for existing drugs. *Nature reviews. Drug discovery*, **3**, 673-
26 683.
- 27 10. Bertolini, F., Sukhatme, V.P. and Bouche, G. (2015) Drug repurposing in
28 oncology--patient and health systems opportunities. *Nat Rev Clin Oncol*, **12**,
29 732-742.
- 30 11. Sleire, L., Forde, H.E., Netland, I.A., Leiss, L., Skeie, B.S. and Enger, P.O.
31 (2017) Drug repurposing in cancer. *Pharmacol Res*, **124**, 74-91.
- 32 12. van't Veer, L.J. and Bernards, R. (2008) Enabling personalized cancer medicine
33 through analysis of gene-expression patterns. *Nature*, **452**, 564-570.
- 34 13. Subramanian, A., Narayan, R., Corsello, S.M., Peck, D.D., Natoli, T.E., Lu, X.,
35 Gould, J., Davis, J.F., Tubelli, A.A., Asiedu, J.K. *et al.* (2017) A Next
36 Generation Connectivity Map: L1000 Platform and the First 1,000,000 Profiles.
37 *Cell*, **171**, 1437-1452 e1417.
- 38 14. van Noort, V., Scholch, S., Iskar, M., Zeller, G., Ostertag, K., Schweitzer, C.,
39 Werner, K., Weitz, J., Koch, M. and Bork, P. (2014) Novel drug candidates for
40 the treatment of metastatic colorectal cancer through global inverse gene-
41 expression profiling. *Cancer research*, **74**, 5690-5699.
- 42 15. Chen, B., Ma, L., Paik, H., Sirota, M., Wei, W., Chua, M.S., So, S. and Butte,
43 A.J. (2017) Reversal of cancer gene expression correlates with drug efficacy and
44 reveals therapeutic targets. *Nat Commun*, **8**, 16022.
- 45 16. Lee, H., Kang, S. and Kim, W. (2016) Drug Repositioning for Cancer Therapy
46 Based on Large-Scale Drug-Induced Transcriptional Signatures. *PLoS One*, **11**,

- 1 e0150460.
- 2 17. Ten Hagen, K.G., Fritz, T.A. and Tabak, L.A. (2003) All in the family: the
3 UDP-GalNAc:polypeptide N-acetylgalactosaminyltransferases. *Glycobiology*,
4 **13**, 1R-16R.
- 5 18. Wagner, K.W., Punnoose, E.A., Januario, T., Lawrence, D.A., Pitti, R.M.,
6 Lancaster, K., Lee, D., von Goetz, M., Yee, S.F., Totpal, K. *et al.* (2007) Death-
7 receptor O-glycosylation controls tumor-cell sensitivity to the proapoptotic
8 ligand Apo2L/TRAIL. *Nat Med*, **13**, 1070-1077.
- 9 19. Wu, C., Shan, Y., Liu, X., Song, W., Wang, J., Zou, M., Wang, M. and Xu, D.
10 (2009) GalNAc-T14 may be involved in regulating the apoptotic action of
11 IGFBP-3. *J Biosci*, **34**, 389-395.
- 12 20. Song, K.H., Park, M.S., Nandu, T.S., Gadad, S., Kim, S.C. and Kim, M.Y.
13 (2016) GALNT14 promotes lung-specific breast cancer metastasis by
14 modulating self-renewal and interaction with the lung microenvironment. *Nat*
15 *Commun*, **7**, 13796.
- 16 21. Huanna, T., Tao, Z., Xiangfei, W., Longfei, A., Yuanyuan, X., Jianhua, W.,
17 Cuifang, Z., Manjing, J., Wenjing, C., Shaochuan, Q. *et al.* (2015) GALNT14
18 mediates tumor invasion and migration in breast cancer cell MCF-7. *Mol*
19 *Carcinog*, **54**, 1159-1171.
- 20 22. Wang, R., Yu, C., Zhao, D., Wu, M. and Yang, Z. (2013) The mucin-type
21 glycosylating enzyme polypeptide N-acetylgalactosaminyltransferase 14
22 promotes the migration of ovarian cancer by modifying mucin 13. *Oncol Rep*,
23 **30**, 667-676.
- 24 23. Kwon, O.S., Oh, E., Park, J.R., Lee, J.S., Bae, G.Y., Koo, J.H., Kim, H., Choi,
25 Y.L., Choi, Y.S., Kim, J. *et al.* (2015) GalNAc-T14 promotes metastasis through
26 Wnt dependent HOXB9 expression in lung adenocarcinoma. *Oncotarget*, **6**,
27 41916-41928.
- 28 24. Shan, J., Liu, Y., Wang, Y., Li, Y., Yu, X. and Wu, C. (2018) GALNT14
29 Involves the Regulation of Multidrug Resistance in Breast Cancer Cells. *Transl*
30 *Oncol*, **11**, 786-793.
- 31 25. De Mariano, M., Gallesio, R., Chierici, M., Furlanello, C., Conte, M., Garaventa,
32 A., Croce, M., Ferrini, S., Tonini, G.P. and Longo, L. (2015) Identification of
33 GALNT14 as a novel neuroblastoma predisposition gene. *Oncotarget*, **6**, 26335-
34 26346.
- 35 26. Soria, J.C., Mark, Z., Zatloukal, P., Szima, B., Albert, I., Juhasz, E., Pujol, J.L.,
36 Kozielski, J., Baker, N., Smethurst, D. *et al.* (2011) Randomized phase II study
37 of dulanermin in combination with paclitaxel, carboplatin, and bevacizumab in
38 advanced non-small-cell lung cancer. *J Clin Oncol*, **29**, 4442-4451.
- 39 27. Lamb, J., Crawford, E.D., Peck, D., Modell, J.W., Blat, I.C., Wrobel, M.J.,
40 Lerner, J., Brunet, J.P., Subramanian, A., Ross, K.N. *et al.* (2006) The
41 Connectivity Map: using gene-expression signatures to connect small molecules,
42 genes, and disease. *Science*, **313**, 1929-1935.
- 43 28. Levy, L. and Hill, C.S. (2005) Smad4 dependency defines two classes of
44 transforming growth factor {beta} (TGF- β) target genes and distinguishes
45 TGF- β -induced epithelial-mesenchymal transition from its antiproliferative
46 and migratory responses. *Molecular and cellular biology*, **25**, 8108-8125.
- 47 29. Tsherniak, A., Vazquez, F., Montgomery, P.G., Weir, B.A., Kryukov, G.,

- 1 Cowley, G.S., Gill, S., Harrington, W.F., Pantel, S., Krill-Burger, J.M. *et al.*
2 (2017) Defining a Cancer Dependency Map. *Cell*, **170**, 564-576 e516.
- 3 30. Stern, H.M., Padilla, M., Wagner, K., Amler, L. and Ashkenazi, A. (2010)
4 Development of immunohistochemistry assays to assess GALNT14 and FUT3/6
5 in clinical trials of dulanermin and drozitumab. *Clin Cancer Res*, **16**, 1587-1596.
- 6 31. Gross, B.J., Swoboda, J.G. and Walker, S. (2008) A strategy to discover
7 inhibitors of O-linked glycosylation. *J Am Chem Soc*, **130**, 440-441.
- 8 32. Hang, H.C., Yu, C., Ten Hagen, K.G., Tian, E., Winans, K.A., Tabak, L.A. and
9 Bertozzi, C.R. (2004) Small molecule inhibitors of mucin-type O-linked
10 glycosylation from a uridine-based library. *Chem Biol*, **11**, 337-345.
- 11 33. Gandolfi, S., Laubach, J.P., Hideshima, T., Chauhan, D., Anderson, K.C. and
12 Richardson, P.G. (2017) The proteasome and proteasome inhibitors in multiple
13 myeloma. *Cancer Metastasis Rev*, **36**, 561-584.
- 14 34. Maggiora, G., Vogt, M., Stumpfe, D. and Bajorath, J. (2014) Molecular
15 similarity in medicinal chemistry. *J Med Chem*, **57**, 3186-3204.
- 16 35. Groll, M., Berkers, C.R., Ploegh, H.L. and Ovaas, H. (2006) Crystal structure of
17 the boronic acid-based proteasome inhibitor bortezomib in complex with the
18 yeast 20S proteasome. *Structure*, **14**, 451-456.
- 19 36. Wakefield, L.M. and Roberts, A.B. (2002) TGF-beta signaling: positive and
20 negative effects on tumorigenesis. *Curr Opin Genet Dev*, **12**, 22-29.
- 21 37. Padua, D. and Massague, J. (2009) Roles of TGFbeta in metastasis. *Cell Res*, **19**,
22 89-102.
- 23 38. Li, A.M., Tian, A.X., Zhang, R.X., Ge, J., Sun, X. and Cao, X.C. (2013)
24 Protocadherin-7 induces bone metastasis of breast cancer. *Biochem Biophys Res*
25 *Commun*, **436**, 486-490.
- 26 39. Moon, Y.W., Rao, G., Kim, J.J., Shim, H.S., Park, K.S., An, S.S., Kim, B.,
27 Steeg, P.S., Sarfaraz, S., Changwoo Lee, L. *et al.* (2015) LAMC2 enhances the
28 metastatic potential of lung adenocarcinoma. *Cell Death Differ*, **22**, 1341-1352.
- 29 40. Zhou, X., Updegraff, B.L., Guo, Y., Peyton, M., Girard, L., Larsen, J.E., Xie,
30 X.J., Zhou, Y., Hwang, T.H., Xie, Y. *et al.* (2017) Dissecting the Role of
31 PCDH7, an Oncogenic Cell Surface Receptor, in Non-Small Cell Lung
32 Cancer. *Journal of Thoracic Oncology*, **12**, S1542.
- 33 41. Huang, D., Du, C., Ji, D., Xi, J. and Gu, J. (2017) Overexpression of LAMC2
34 predicts poor prognosis in colorectal cancer patients and promotes cancer cell
35 proliferation, migration, and invasion. *Tumour Biol*, **39**, 1010428317705849.
- 36 42. Gupta, G.P. and Massague, J. (2006) Cancer metastasis: building a framework.
37 *Cell*, **127**, 679-695.
- 38 43. Jahchan, N.S., Dudley, J.T., Mazur, P.K., Flores, N., Yang, D., Palmerton, A.,
39 Zmoos, A.F., Vaka, D., Tran, K.Q., Zhou, M. *et al.* (2013) A drug repositioning
40 approach identifies tricyclic antidepressants as inhibitors of small cell lung
41 cancer and other neuroendocrine tumors. *Cancer Discov*, **3**, 1364-1377.
- 42 44. Zeniya, M., Mori, T., Yui, N., Nomura, N., Mandai, S., Isobe, K., Chiga, M.,
43 Sohara, E., Rai, T. and Uchida, S. (2017) The proteasome inhibitor bortezomib
44 attenuates renal fibrosis in mice via the suppression of TGF-beta1. *Sci Rep*, **7**,
45 13086.
- 46 45. Chang, T.P., Poltoratsky, V. and Vancurova, I. (2015) Bortezomib inhibits
47 expression of TGF-beta1, IL-10, and CXCR4, resulting in decreased survival

- 1 and migration of cutaneous T cell lymphoma cells. *J Immunol*, **194**, 2942-2953.
- 2 46. Padua, D., Zhang, X.H., Wang, Q., Nadal, C., Gerald, W.L., Gomis, R.R. and
3 Massague, J. (2008) TGFbeta primes breast tumors for lung metastasis seeding
4 through angiopoietin-like 4. *Cell*, **133**, 66-77.
- 5 47. Wagle, M.C., Kirouac, D., Klijn, C., Liu, B., Mahajan, S., Junttila, M., Moffat,
6 J., Merchant, M., Huw, L., Wongchenko, M. *et al.* (2018) A transcriptional
7 MAPK Pathway Activity Score (MPAS) is a clinically relevant biomarker in
8 multiple cancer types. *Npj Precis Oncol*, **2**.
- 9 48. Argyriou, A.A., Iconomou, G. and Kalofonos, H.P. (2008) Bortezomib-induced
10 peripheral neuropathy in multiple myeloma: a comprehensive review of the
11 literature. *Blood*, **112**, 1593-1599.
- 12 49. Oprea, T.I. and Overington, J.P. (2015) Computational and Practical Aspects of
13 Drug Repositioning. *Assay Drug Dev Technol*, **13**, 299-306.
- 14 50. Iorio, F., Rittman, T., Ge, H., Menden, M. and Saez-Rodriguez, J. (2013)
15 Transcriptional data: a new gateway to drug repositioning? *Drug Discov Today*,
16 **18**, 350-357.
17

Figure. 1

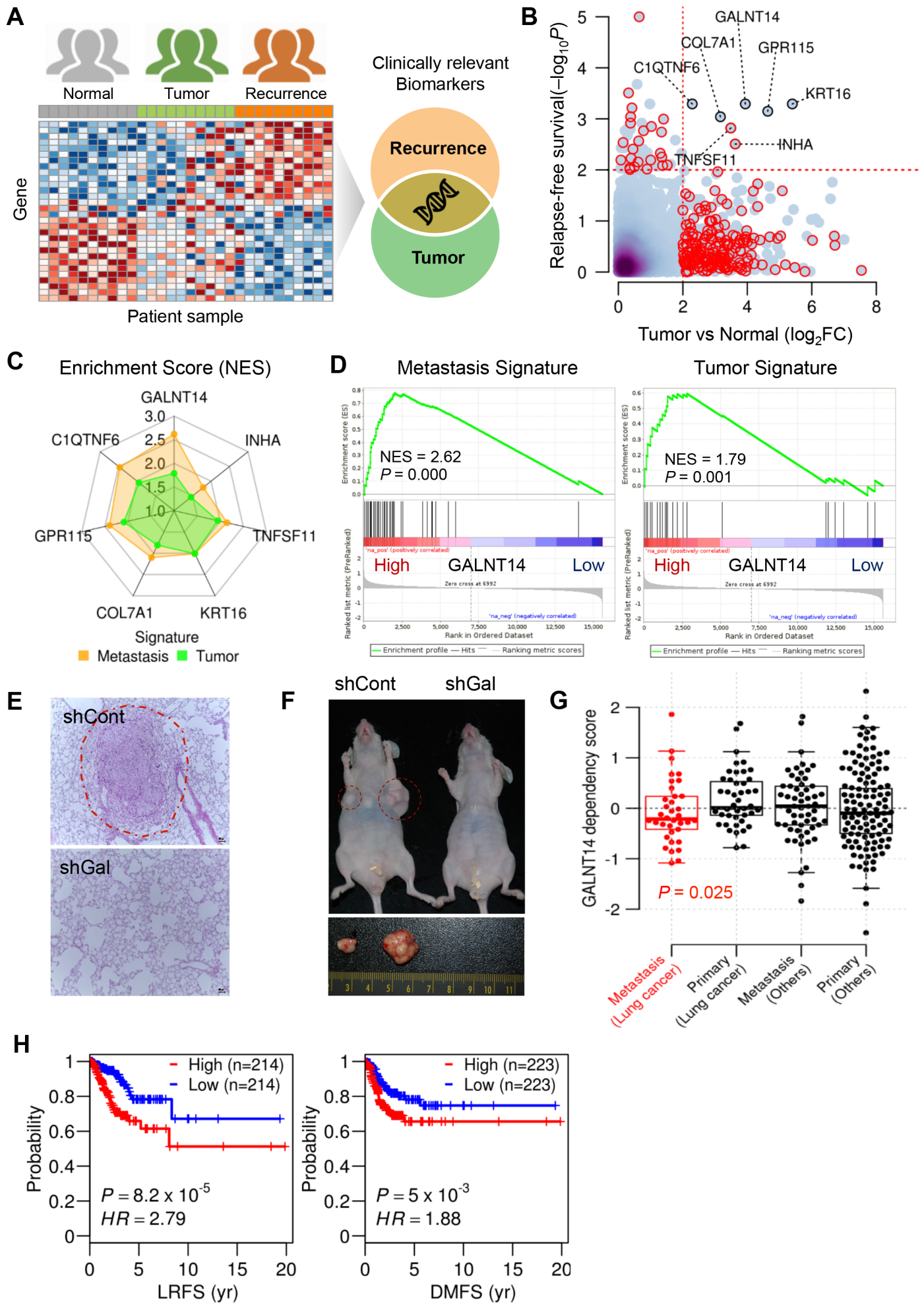


Figure. 2

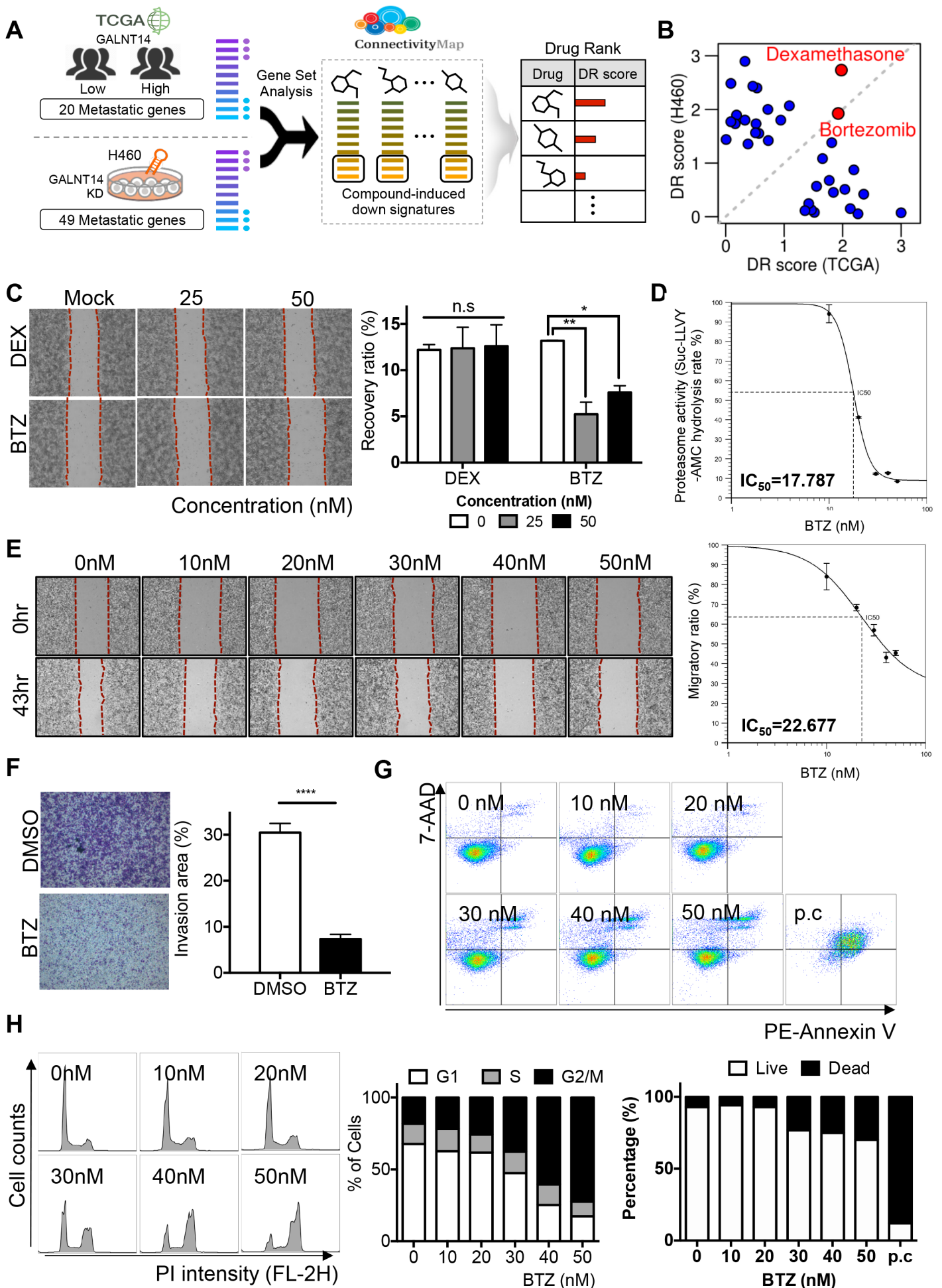
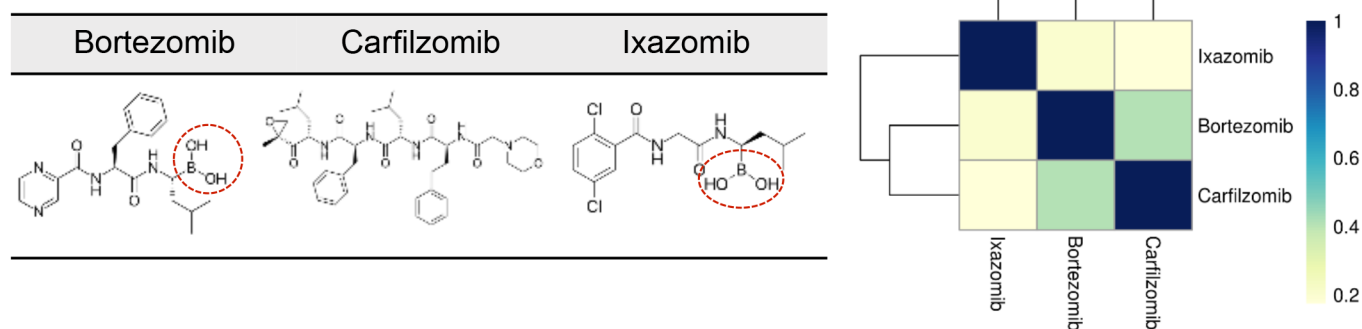
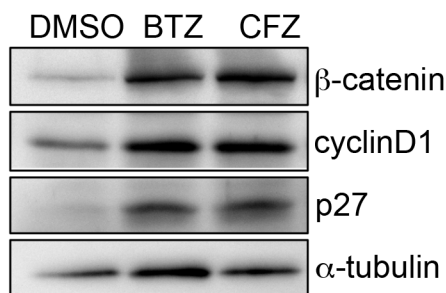


Figure. 3

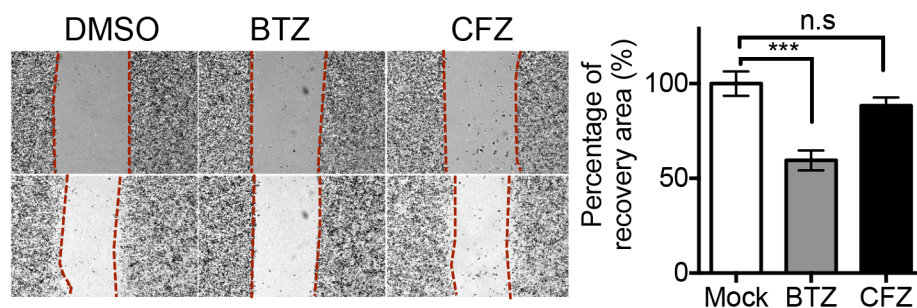
A



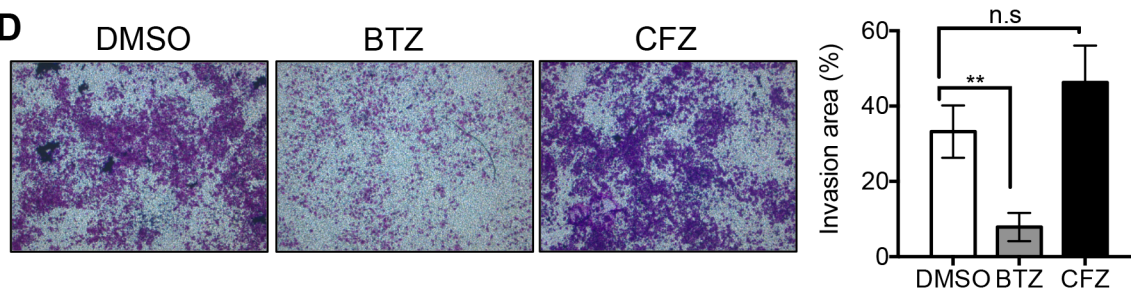
B



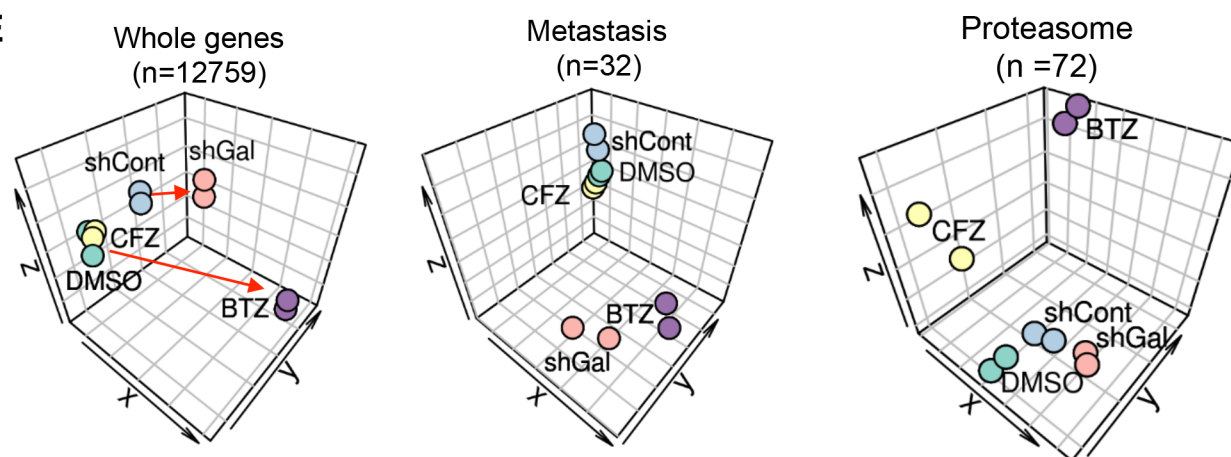
C



D



E



F

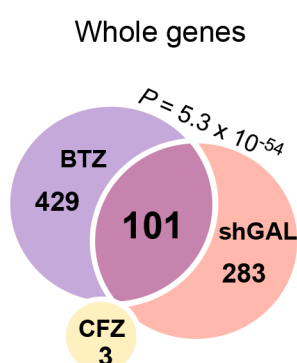
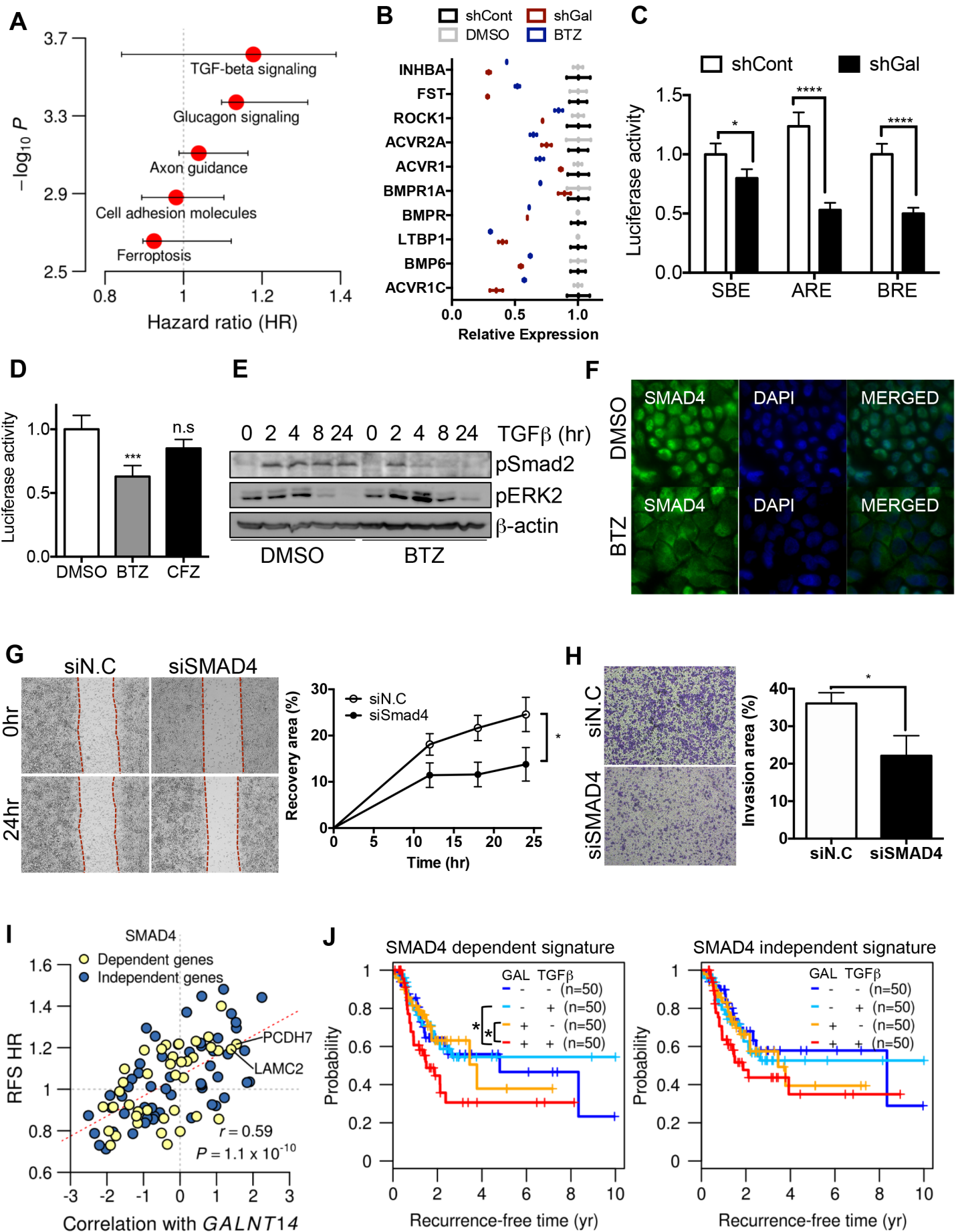


Figure 4



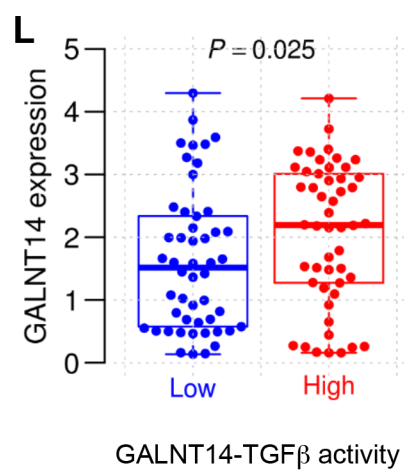
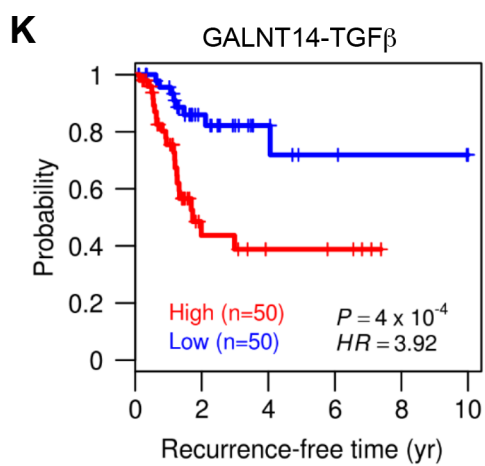


Figure. 5

